South Pole–Aitken Basin Ejecta Inferred from Crustal Thickness. P.B. James[1], J.T. Keane[2], and J.S. Lee[1,3]. [1]Department of Geosciences, Baylor University, Waco, TX 76798 (P_James@baylor.edu), [2]Jet Propulsion Laboratory, California Institute of Technology, [3]Center for Astrophysics, Space Physics & Engineering Research, Baylor University.

Introduction: The South Pole–Aitken (SPA) basin-forming impact event likely excavated large volumes of the Moon's crust and mantle, and the resulting ejecta deposits may have reached thicknesses of many kilometers [1]. Thus, SPA basin ejecta played a major role in the development of the Moon's megaregolith. The SPA basin is understood to have been formed by an oblique impact, and the orientation of the basin's elliptical shape has been constrained within a few degrees by topography and crustal thickness [2]. However, the direction of the impact is not known. Magnetic anomalies at the northern rim could imply an approach from the south [3], but nearside mare volcanism could be explained by an approach from the north [4]. The thickest ejecta deposits likely exist in the downrange direction; consequently, ejecta distribution may offer new insight into the approach direction of the impactor.

This abstract and a companion abstract ([5], #1477) investigate plausible distributions of SPA ejecta based on the GRAIL-derived crustal thickness with slightly different methodologies.

Methods: The central presupposition of this work is that the distribution of ejecta is largely (but not exclusively) symmetric across the basin's major axis. We start with a map of crustal thickness, $C(\theta,\phi)$, with 73 basins (not including SPA) removed to plausibly infer the crustal thickness map that immediately post-dated the formation of the SPA basin. The methodology of this basin removal is described in more detail in [6] and in our companion abstract [5]. With this basin-free map, we decompose the Moon's crustal thickness into symmetric $(S(\theta,\phi))$ and anti-symmetric $(A(\theta,\phi))$ maps:

$$C(\theta,\phi) = S(\theta,\phi) + A(\theta,\phi)$$

The symmetry axis is defined by the major axis of the SPA basin, which has a tilt of 16°–19° west of north based on several analyses of crustal thickness, topography, rim scarps, and composition [2,7]. As noted above, we don't expect an ejecta distribution to be perfectly symmetric. In particular, symmetry is expected less at length scales much smaller than the length scale of the basin itself. Consequently, we can define a "semi-symmetric" (SS) distribution of crustal thickness that allows short-wavelength asymmetry:

$$SS(\theta,\phi) = S(\theta,\phi) + \lambda_l A(\theta,\phi)$$

The coefficient λ_l attenuates the asymmetric crustal thickness distribution:

$$\lambda_l = \exp\left(-\frac{\pi R}{al}\right)$$

where R is the Moon's radius, a is the semimajor axis of SPA, and l is spherical harmonic degree. We furthermore reduced the degree-2 portion of the semi-symmetric distribution by half to allow for the possibility of a degree-2 figure that preceded SPA.

The thickness of the ejecta may then be derived from the semi-symmetric crustal thickness distribution shown above. Presuming the total volume of emplaced ejecta to be 8×10^7 cubic kilometers [2], we find that the semi-symmetric crustal thickness in excess of 37

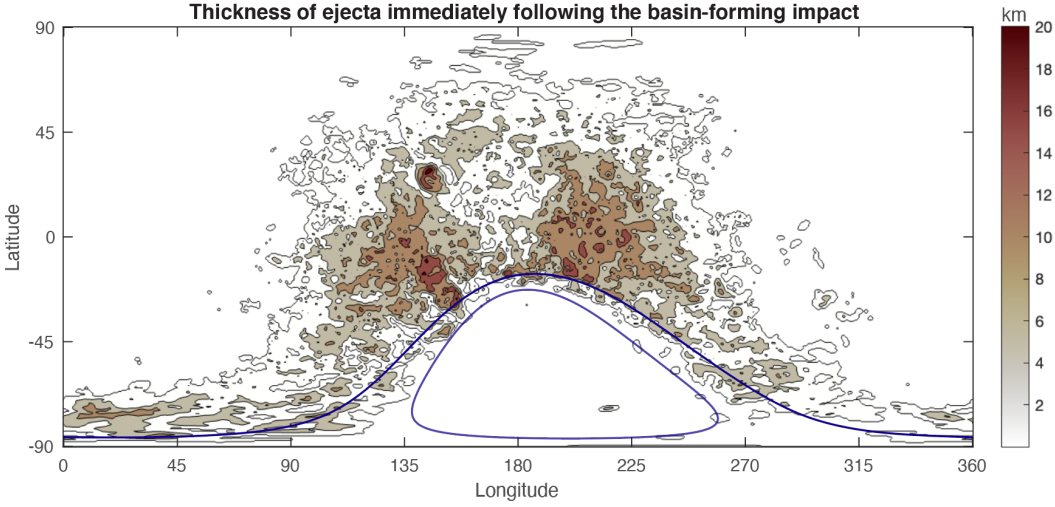

Figure 1: Inferred thickness of SPA ejecta under the assumption of semi-symmetry. Black curves indicate the inner & outer rim locations [2]. The "bilbao" color map was created by [8].

kilometers is equivalent to this prescribed volume. We take this excess volume to be ejecta.

Results: Under the assumption of semi-symmetry, we infer the ejecta thickness distribution shown in Figure 1. Note that this corresponds to the thickness of ejecta at a specific point in time: before any subsequent basins were superimposed on the ejecta blanket, but after horizontal sliding and viscous relaxation of ejecta materials ceased. In particular, crust may have relaxed inward toward the basin center in the hours after an impact [9]. Therefore, Figure 1 may underrepresent the instantaneous distribution of ejecta in the vicinity of the basin's rims.

Ejecta exists almost continuously around the periphery of the basin, reaching thicknesses of >10 kilometers in some portions of the far-side highlands. Ejecta is especially concentrated in two prominent lobes north of the basin, straddling the major axis of the SPA basin's elliptical shape. Previous iSALE models have suggested that most of the deposited ejecta from the SPA basin-forming impact event should be found down-range from the basin [1]. Therefore, the ejecta distribution shown in Figure 1 strongly implies that the SPA basin was formed by an oblique impact approaching from the south.

SPA ejecta appears to exist throughout the far-side highlands. Even in regions where SPA ejecta did not substantially thicken the crust, ejecta materials likely contribute to the average composition of present-day megaregolith [10], i.e., noritic anorthosite. This is consistent with excavation of a pyroxenite mantle by the basin-forming impact [1].

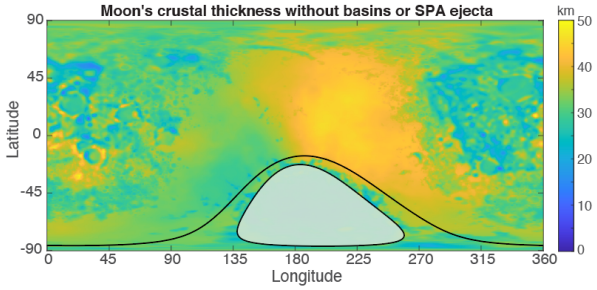

Figure 2: Crustal thickness map with basins and the SPA ejecta blanket removed. The basin interior is masked.

When we remove SPA ejecta from the basin-free crustal thickness map, we get a new crustal thickness map (Figure 2). This map shows the plausible crustal thickness immediately prior to the formation of the SPA basin. Unlike our companion abstract [5], the semi-symmetry method does not fully explain the existence of the thickest crust in the far-side highlands. However, Figure 2 shows that the extent of "thick" crust (defined here to be >40 km) was more geographically limited than present-day crustal thickness. Our model predicts that most of the highland crust west of the 180°E meridian had thicknesses close to the global mean, and that the relatively thick crust in those locations today is largely due to SPA ejecta.

Caveats and future work: The fate of SPA's ejecta remains a challenging problem for several reasons, and it is ripe for further inquiry.

Uncertainty of ejecta volume. While we can put a lower bound on the volume of material ejected from SPA based on the deficit of crust in the basin interior, we cannot predict how much of that material was subsequently emplaced on the lunar surface. If we overestimated the total volume of emplaced ejecta, the true ejecta thickness would correspond to one of the positive contours in Figure 1.

How symmetric was SPA ejecta in reality? Our analysis rests on the presupposition that SPA ejecta is largely symmetric. However, our own Figure 2 implies that the pre-existing crust featured long-wavelength thickness variations of >10 km at the time of impact. Crustal thickness variations may conceivably influence the distribution of ejecta. If we further relax the assumption of symmetry, the inferred ejecta distribution will approach that of our companion abstract [5].

Sensitivity tests. We plan to implement "sensitivity tests" in which we apply checkerboard ejecta patterns on top of synthetic crustal thickness maps with similar power spectra. This will probe the accuracy and repeatability of our semi-symmetry approach, and it may motivate a refined definition of the attenuation coefficient λ_l.

Complementary investigations. This work has made predictions about the distribution of ejecta materials, which imply variations in composition and megaregolith depth. These inferences could be tested with additional geophysical methods such as spatio-spectral localization.

Acknowledgments: This work was made possible by data sets from the GRAIL mission and the LOLA instrument. These data are hosted on the Planetary Data System (PDS) Geosciences Node.

References: [1] Melosh H.J. et al. (2017) *Geology* 45.12, 1063-1066. [2] James P.B. et al. (2019) *GRL* 46.10, 5100-5106. [3] Wieczorek, M. A., et al. (2012) *Science* 335.6073, 1212-1215. [4] Schultz, P.H. and Crawford D.A. (2011) *GSA Special Papers* 477, 141-159. [5] Keane J.T. et al., *LPSC LIII*, #1477 (this mtg). [6] Matsuyama I. et al. (2021) *Icarus* 358, 114202. [7] Garrick-Bethell I. and Zuber M.T. (2009) *Icarus* 204.2, 399-408. [8] Crameri F. et al. (2020) *Nature communications* 11.1, 1-10. [9] Johnson B.C. et al. (2016) Science 354.6311, 441-444. [10] Richardson J.E. and Abramov O. (2020) *PSJ* 1.1, 2.